Article

Cell Reports

Antibody-Mediated Targeting of Tau In Vivo Does Not Require Effector Function and Microglial Engagement

Graphical Abstract

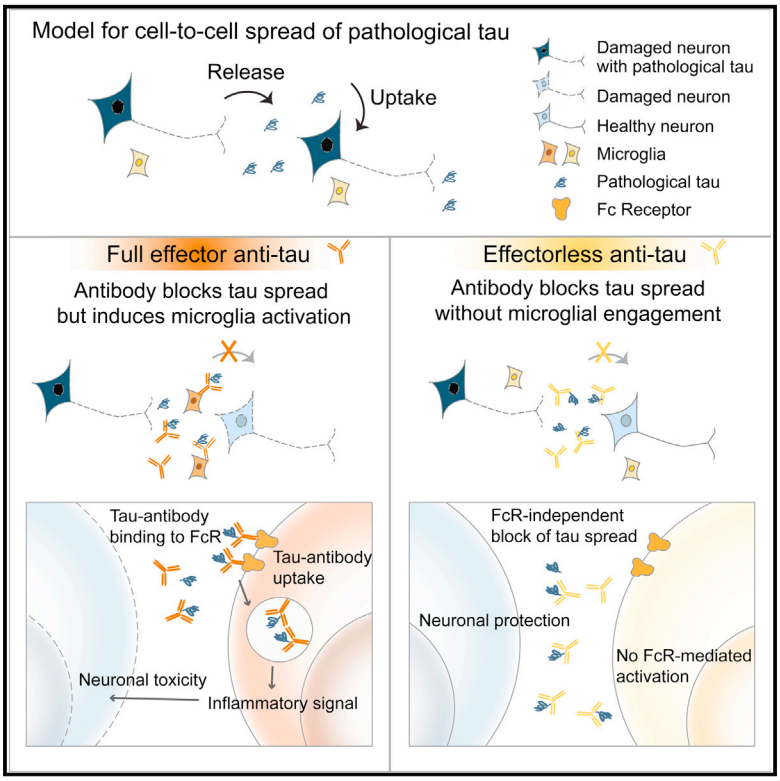

Highlights

- Antibody effector function and microglia engagement are not required for targeting tau
- Full effector and effectorless tau antibodies slow the spread of tau pathology in vivo
- Only effectorless anti-tau protects neurons from toxic tau in the presence of microglia
- Anti-tau with reduced effector function may represent a safer approach to targeting tau

Authors

Seung-Hye Lee, Claire E. Le Pichon, Oskar Adolfsson, ..., Andreas Muhs, Kimberly Scearce-Levie, Gai Ayalon

Correspondence

andreas.muhs@acimmune.com (A.M.), kscearcelevie@gmail.com (K.S.-L.), ayalon.gai@gene.com (G.A.)

In Brief

Lee et al. report that antibody effector function is not required for targeting tau with antibodies in vivo and in cultured neurons. The authors propose that reducing anti-tau effector function may offer a safer approach for targeting tau by avoiding engagement of microglia that may induce inflammatory responses.

Lee et al., 2016, Cell Reports *16*, 1690–1700
August 9, 2016
http://dx.doi.org/10.1016/j.celrep.2016.06.099

OPEN ACCESS
CellPress

Cell Reports
Article

Antibody-Mediated Targeting of Tau In Vivo Does Not Require Effector Function and Microglial Engagement

Seung-Hye Lee,[1,3] Claire E. Le Pichon,[1,3,4] Oskar Adolfsson,[2] Valérie Gafner,[2] Maria Pihlgren,[2] Han Lin,[1] Hilda Solanoy,[1] Robert Brendza,[1] Hai Ngu,[1] Oded Foreman,[1] Ruby Chan,[1,5] James A. Ernst,[1] Danielle DiCara,[1] Isidro Hotzel,[1] Karpagam Srinivasan,[1] David V. Hansen,[1] Jasvinder Atwal,[1] Yanmei Lu,[1] Daniela Bumbaca,[1] Andrea Pfeifer,[2] Ryan J. Watts,[1] Andreas Muhs,[2,*] Kimberly Scearce-Levie,[1,*] and Gai Ayalon[1,*]

[1]Genentech, South San Francisco, CA 94080, USA
[2]AC Immune SA, 1015 Lausanne, Switzerland
[3]Co-first author
[4]Present address: National Institute of Neurological Disorders and Stroke, National Institutes of Health, Bethesda, MD 20892, USA
[5]Present address: Gilead Sciences, Foster City, CA 94404, USA
*Correspondence: andreas.muhs@acimmune.com (A.M.), kscearcelevie@gmail.com (K.S.-L.), ayalon.gai@gene.com (G.A.)
http://dx.doi.org/10.1016/j.celrep.2016.06.099

SUMMARY

The spread of tau pathology correlates with cognitive decline in Alzheimer's disease. In vitro, tau antibodies can block cell-to-cell tau spreading. Although mechanisms of anti-tau function in vivo are unknown, effector function might promote microglia-mediated clearance. In this study, we investigated whether antibody effector function is required for targeting tau. We compared efficacy in vivo and in vitro of two versions of the same tau antibody, with and without effector function, measuring tau pathology, neuron health, and microglial function. Both antibodies reduced accumulation of tau pathology in Tau-P301L transgenic mice and protected cultured neurons against extracellular tau-induced toxicity. Only the full-effector antibody enhanced tau uptake in cultured microglia, which promoted release of proinflammatory cytokines. In neuron-microglia co-cultures, only effectorless anti-tau protected neurons, suggesting full-effector tau antibodies can induce indirect toxicity via microglia. We conclude that effector function is not required for efficacy, and effectorless tau antibodies may represent a safer approach to targeting tau.

INTRODUCTION

Alzheimer's disease (AD) pathology is characterized by amyloid plaques, neurofibrillary tangles (NFTs), extensive neuroinflammation, and neuronal cell death (Glass et al., 2010; Skovronsky et al., 2006). Tau, a cytosolic soluble microtubule-binding protein that is intrinsically unstructured, is the primary constituent of NFTs, where it is found to be hyperphosphorylated and aggregated (Mandelkow and Mandelkow, 2012). Tau tangle pathology is the hallmark of several neurodegenerative diseases collectively termed tauopathies, which include AD, progressive supranuclear palsy (PSP), frontotemporal dementia (FTD), corticobasal degeneration (CBD), Pick's disease, and others, and the causal significance of tau in neurodegeneration is apparent from disease-causing autosomal-dominant tau mutations (Goedert et al., 2012).

Multiple lines of evidence suggest that tau, while typically thought of as an intracellular cytosolic protein, can also be found extracellularly. Tau has been shown to be released by cultured cells via an unconventional mechanism (Chai et al., 2012), extracellular tau has been measured directly in the interstitial fluid in mice (Yamada et al., 2011), and tau is present in human cerebrospinal fluid (CSF), where its concentration is elevated in AD patients (Shaw et al., 2009). The tau-spread hypothesis stipulates that pathological tau can spread from cell to cell via the extracellular environment, thereby propagating disease progression. In support of this idea, the spread of tau pathology has been demonstrated in cultured cells (Kfoury et al., 2012), animal models (de Calignon et al., 2012; Iba et al., 2013; Liu et al., 2012), and AD patients as disease progresses, correlating with cognitive decline (Braak and Braak, 1991, 1995). Approaches utilizing antibodies to target tau have been successful in reducing pathology in tau transgenic mouse models (Boutajangout et al., 2011; Chai et al., 2011; d'Abramo et al., 2013; Yanamandra et al., 2013); however, the mechanisms and possible liabilities of therapeutic approaches using tau antibodies remain poorly understood.

The therapeutic promise of immunotherapy needs to be balanced by potential liabilities associated with immune modulation, particularly in the nervous system (Yu and Watts, 2013). This is apparent from cases where amyloid-β-targeting antibodies have led to vasogenic edema (ARIA-E; amyloid-related imaging abnormalities) (Ostrowitzki et al., 2012; Sperling et al., 2012), a liability that can be mitigated by reducing

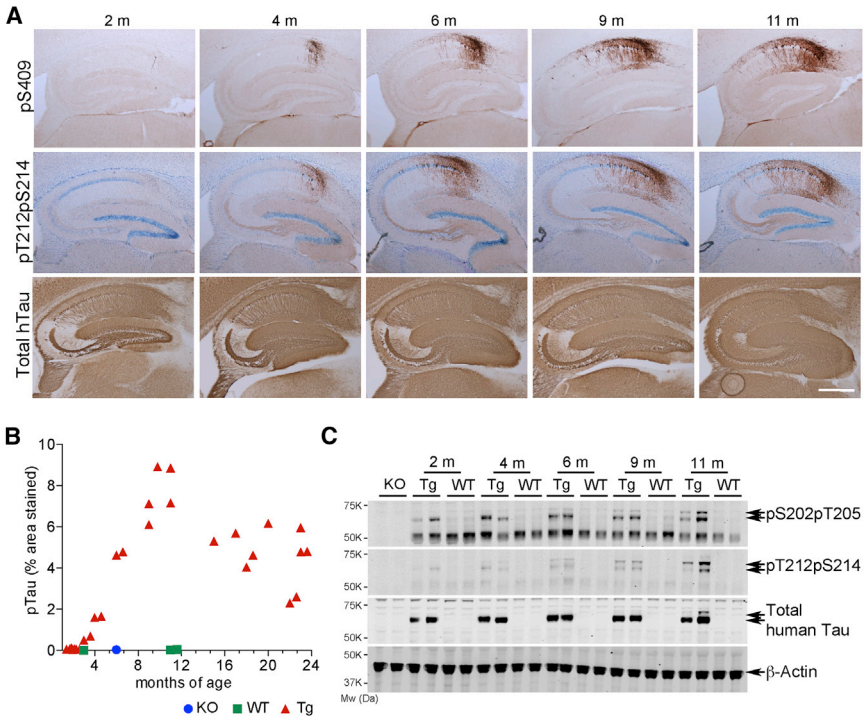

Figure 1. Age-Dependent Spread and Accumulation of Phosphorylated Tau Pathology in the Hippocampus of Tau P301L-Tg Mice

(A) Representative images of P301L-Tg mouse hippocampi of the designated ages stained for S409-phosphorylated tau (PG5 antibody, top panels), T212/S214-phosphorylated tau (pT212/pS214 antibody, middle panels), and total human tau (HT7 antibody, bottom panels). Scale bar, 500 μm.

(B) Quantification of the area of hippocampal pS409-Tau pathology in Tau P301L-Tg (Tg; red), wild-type littermates (WT; green) and tau knockout (KO; blue) mice. Each point is the average percent area stained for three sections from a single animal.

(C) Western blot of brain lysates showed an age-dependent increase in pTau in P301L-Tg mice. Brain lysates from mice of the indicated genotypes and ages were probed for pS202pT205, pT212pS214, human tau-specific (HT7), and β-actin. Paired arrows indicate the molecular weight of human P301L Tau (~60–70 kDa), and the upper arrow of each pair corresponds to hyperphosphorylated Tau.

antibody effector function (Adolfsson et al., 2012). The state of neuroinflammation in AD (reviewed in Wyss-Coray and Rogers, 2012) further exemplifies the need to assess the potential impact of antibody treatment on inflammatory responses, and especially the role effector function may play in these responses, as well as in efficacy.

Effector function, an intrinsic property of an antibody that drives phagocytic and proinflammatory responses, is mediated by antibody interactions with immune cells via Fcγ receptors (FcγRs) and complement, and these interactions can be modulated by mutations in the immunoglobulin G (IgG) Fc region (Leabman et al., 2013). The question of whether effective tau immunotherapeutics require effector function has not previously been investigated. Indeed, it may be that antibody binding of tau is sufficient to prevent it from spreading, without the additional requirement for effector function, thus avoiding potential pro-inflammatory side effects.

In this study, utilizing phospho-serine-409 tau antibodies with effector variants, we explored the mechanisms underlying tau antibody efficacy, including whether antibody effector function is required to reduce accumulation of tau pathology in vivo. We further investigated the cellular implications of treatment with effector function variants of anti-tau on cultured neurons and microglia. We show that effector function is not required for efficacy in vivo and that, although full effector function anti-tau promotes microglial uptake of extracellular tau, it also elicits microglial release of proinflammatory cytokines that could have deleterious effects on neurons. Our results suggest that attenuation of antibody effector function may offer a safer route for targeting tau with antibodies and shed light on the mechanism of action of tau antibodies.

RESULTS

Age-Dependent Accumulation of Phospho-tau Pathology in Tau P301L-Tg Mice

We first characterized the accumulation of tau pathology by immunohistochemistry (IHC) and biochemistry in Tau P301L-Tg mice (Götz et al., 2001), a tauopathy mouse model that expresses human tau harboring a mutation that causes frontotemporal dementia. Hippocampal phospho-tau pathology increases with age in this model, beginning in the subiculum and CA1 regions at 2 months of age and progressing toward CA2/3 and reaching a maximum burden at 12 months (Figures 1A and 1B). Western blots of brain lysates confirmed age-dependent increases in hyperphosphorylated tau (Figure 1C). Using both methods, we detected age-related increases in a range of phospho-tau epitopes, including pS202pT205, pT212pS214, and pS409 (Figures 1A and 1C).

Generation and Characterization of Anti-pS409-Tau Full Effector and Effectorless Antibodies

Phosphorylated serine-409 is a phospho-tau epitope that has been reported to appear early in tangle formation and persist in NFTs (Kimura et al., 1996). We generated a murine therapeutic antibody targeting pS409-Tau, confirming its phospho-epitope specificity and its reactivity to pathological human tau by ELISA, western blot, and IHC (Figures 2A–2D and S1). An effectorless version of the full effector recombinant murine IgG2a antibody was engineered by introducing the D265A and N297G (DANG) mutations in the Fc region, which, combined, abolish binding to FcγRs (Couch et al., 2013).

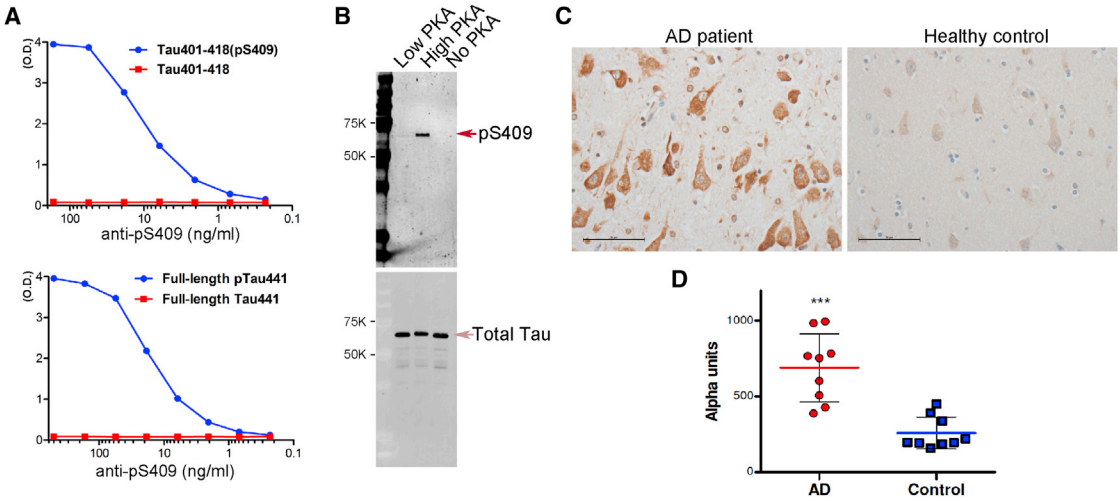

Figure 2. A Murine Therapeutic Antibody Specific to S409-Phosphorylated Tau Reacts with Pathological Tau from Human AD Patients

(A) Selectivity of the antibody to phospho-S409 tau was confirmed by ELISA against phospho- and non-phospho-peptides (top) as well as recombinant human tau nonphosphorylated or phosphorylated in vitro with PKA (bottom).

(B) Western blot using full-length Tau protein phosphorylated with PKA at 2,088 U/ml (Low PKA) or 12,525 U/ml (High PKA) or unphosphorylated (No PKA). pS409 antibody specifically detected the phosphorylated tau (red arrow). Total tau bands (pink arrow) were visualized with a pan-tau antibody (Tau-5).

(C) Cortical brain sections from Alzheimer patient and healthy control stained with anti-pS409 antibody by immunohistochemistry. Scale bars, 50 μm.

(D) Detection of pS409-Tau in human brain S1 homogenates using biotinylated the pS409-Tau antibody. A significant difference ($p < 0.0001$, Mann-Whitney test) was observed between AD and control brains.

Effector Function Is Not Required for Targeting Spread of Tau Pathology In Vivo

Tau P301L-Tg mice were injected intraperitoneally once weekly for 3 months starting at 3 months of age with either the full effector (WT) or effectorless (DANG) pS409-Tau antibodies or a control IgG2a antibody. Plasma and perfused brains were harvested for analyses 24 hr after the last dose, antibody concentrations were measured (Figure S2), and right hemispheres were processed for histopathology. A significant reduction in hippocampal tau pathology was observed in mice treated with both WT and DANG pS409-Tau antibodies (Figures 3A and 3B). To biochemically assess the effect of antibody treatment on tau pathology, hippocampi from the left hemispheres were homogenized and fractionated for western blot analysis of insoluble phospho-tau. Both WT and DANG anti-pS409-Tau variants significantly lowered insoluble levels of phospho-tau, with no significant difference between the antibodies (Figures 3C–3E).

Importantly, 3-month dosing of older animals starting at 11.5 months of age, when pathology is already maximally established (see Figure 1B) did not reduce hippocampal tau pathology (Figure S3). Taken together, these results suggest that in vivo, tau antibodies do not clear existing intra-neuronal pathology but rather slow down the spread of pathology in earlier stages of propagation. Because in vivo efficacy is independent of antibody effector function status, the data further suggest that tau antibodies can be efficacious without binding to FcγRs.

pS409-Tau Antibodies Protect Cultured Neurons from Tau-Induced Toxicity Independent of Effector Function Status

To gain mechanistic insight into anti-tau function, we tested the capacity of our tau antibodies to protect cultured neurons from tau-induced toxicity. We phosphorylated recombinant human tau in vitro with protein kinase A (PKA), which phosphorylates tau on S409 (Jicha et al., 1999), and oligomerized the phospho-tau protein (Figure S4). When added to the media of cultured mouse hippocampal neurons, oligo-pTau caused toxicity in a concentration-dependent manner (Figures S5A and S5B), visualized as fragmentation of MAP2 staining along neurites. Oligomeric tau that was not PKA phosphorylated also induced neuronal toxicity, comparable to oligo-pTau (Figure S5C). Monomeric tau, on the other hand, did not cause any noticeable toxicity to cultured neurons, even at high concentrations (Figure S5C). For subsequent experiments, a high oligo-pTau concentration (500 nM) was used to ensure robust toxicity. We treated cultured neurons with vehicle control, oligo-pTau, or oligo-pTau plus equimolar concentration of anti-pS409-Tau WT, anti-pS409-Tau DANG, or IgG2a-control. Automated quantification of MAP2 fragmentation showed that oligo-pTau-induced toxicity is blocked in the presence of either tau antibody variant, irrespective of effector function status (Figures 4A and 4D). In cultures treated with oligo-pTau or oligo-pTau plus IgG2a-control, tau staining was observed in both neurons as well as non-neuronal cells (Figure 4B). In contrast, neurons that were treated with oligo-pTau together with tau antibodies showed minimal tau staining in neurons, seen as lack of staining overlapping with MAP2-positive neurons; however, there appeared to be some tau staining in non-neuronal cells. Anti-Tau or control antibodies were detected in non-neuronal cells but not in neurons (Figure 4C). Both WT and DANG antibodies showed comparable dose-dependent protection of cultured neurons exposed to 500 nM oligo-pTau (Figures S5D and S5E).

Our data indicate that tau antibodies may prevent internalization of extracellular tau by neurons, although some published

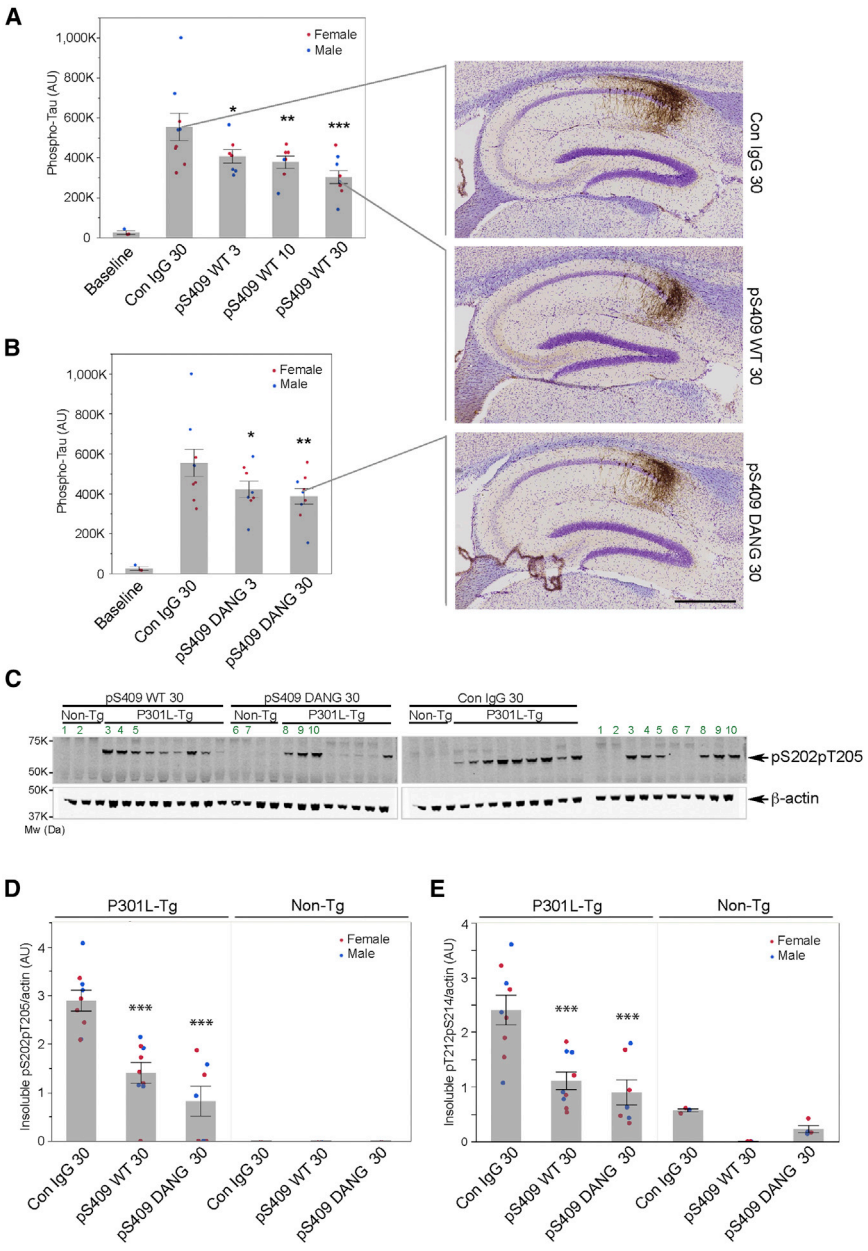

Figure 3. Reduction in Hippocampal Tau Pathology in P301L-Tg Mice following 3 Months Weekly Intraperitoneal Dosing with Anti-pS409

3-month-old P301L-Tg mice and WT controls were dosed weekly with anti-pS409 tau antibodies for 3 months.

(A) Significant reduction in pS409 tau staining in P301L-Tg mice dosed with the full effector pS409 WT antibody was observed in all dose groups (ANOVA for dose level, $p = 0.008$; comparisons to 30 mg/kg control IgG group by two-tailed Student's t test; *$p = 0.0281$, **$p = 0.0091$, and ***$p = 0.0002$). Representative images of mice treated with 30 mg/kg control antibody (above) and 30 mg/kg anti-pS409 WT antibody (below), corresponding to individuals as indicated.

(B) Significant reduction of pS409 tau staining in P301L-Tg mice dosed with the effectorless pS409 DANG antibody in both dose groups (ANOVA for dose level, $p = 0.048$; compared to 30 mg/kg control IgG group; 2-tailed Student's t test, *$p = 0.0395$, **$p = 0.0083$) Representative image of 30 mg/kg anti-pS409 DANG-treated mouse, corresponding to the individual mouse data point, as indicated. p values were calculated by two-tailed Student's t test. For ease of comparison, graphs in (A) and (B) show the same baseline and control-IgG-treated animals. In (A) and (B), each point represents an averaged quantification of three or four sections per animal measured for integrated signal intensity of pS409 tau within the hippocampal ROI. Baseline indicates transgenic mice at the start of the study (3 months old) that were never treated. No pS409 tau signal and no antibody effect were detected in WT littermate animals (not depicted).

(C–E) Anti-pS409-Tau reduces accumulation of insoluble phosphorylated tau in hippocampal lysates of P301L-Tg mice following 3-month weekly intraperitoneal dosing. Western blot data from insoluble fractions of hippocampal homogenates from the same mice treated with 30 mg/kg antibodies shown in (A) and (B). In (C), lanes numbered in green indicate samples loaded twice for gel factor normalization. In (D) and (E), graphs represent densitometric quantification of normalized band intensities of phospho-tau to β-actin. Treatment with both full effector function IgG2a WT and effectorless DANG antibodies resulted in comparable and significant reduction in phospho-tau (pS202pT205 and pT212pS214) levels in insoluble fractions (P2; see Experimental Procedures).

***$p < 0.001$, two-tailed Student's t test versus control IgG treated. Con IgG, control IgG2a antibody; pS409 WT, anti-pS409 IgG2a WT antibody; pS409 DANG, anti-pS409 IgG2a DANG mutant; numbers (3, 10, and 30) after Con IgG, pS409 WT, and pS409 DANG represent milligrams per kilogram of antibody administered. See Table S1 for detailed description and count of animals used in this study. AU, arbitrary units. Error bars, SEM; scale bar, 500 μm.

studies propose that neurons internalize tau antibodies via FcγRs (Congdon et al., 2013). We found no evidence of neuronal expression of FcγRs 1–3 in the online public transcriptome database of the wild-type (WT) mouse CNS (http://web.stanford.edu/group/barres_lab/brain_rnaseq.html) (Zhang et al., 2014). To address the possibility that under neurodegenerative conditions neurons aberrantly express FcγRs, we sorted neurons and microglia from adult Tau P301L-Tg and non-transgenic littermates and assessed the expression of FcγRs 1–3 by qPCR. For both genotypes, we detected RNA transcripts of FcγRs in microglia but not in neurons (Figure 5A). Enrichment of neurons and microglia following cell sorting was confirmed by the selective detection of the cell-specific RNA transcripts Grin1 and Cx3Cr1, respectively (Figure 5B). We also stained cultured hippocampal neurons with the anti-FcγR antibody against CD16/CD32 and detected no signal; however, microglia added to the neuronal culture showed clear FcγR staining (Figure 5C). These results suggest that tau antibodies

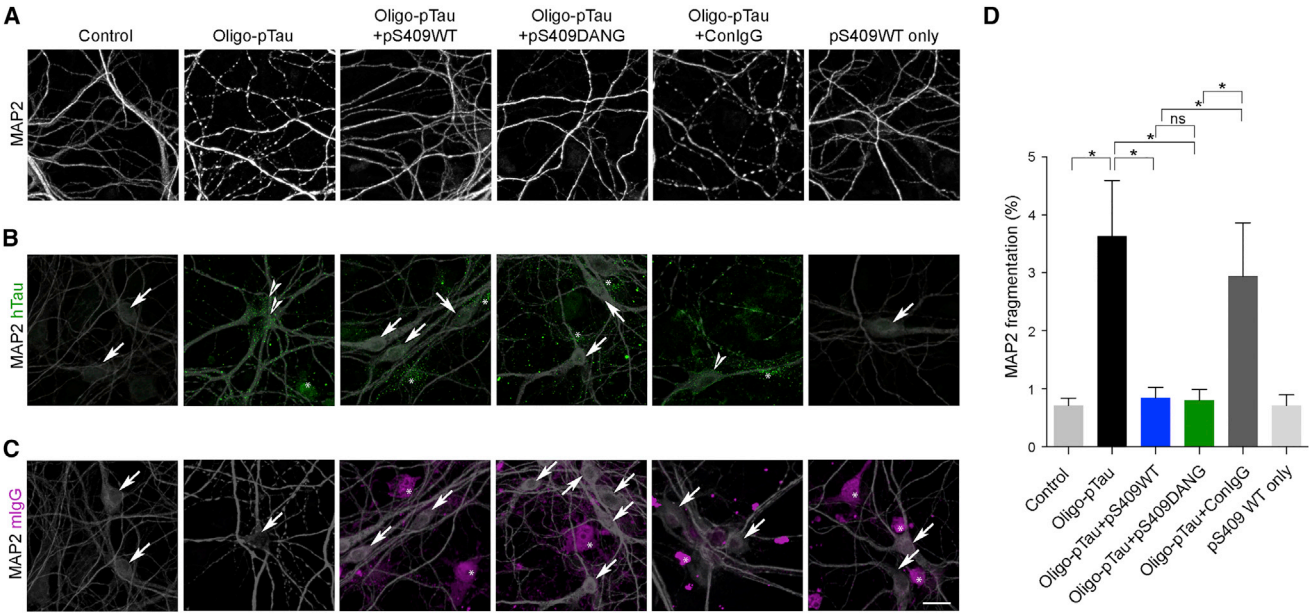

Figure 4. pS409 Tau Antibodies Protect Cultured Hippocampal Neurons from Toxicity Induced by Recombinant Oligomeric Phospho-tau Independent of Effector Function

(A–C) Primary cultured hippocampal neurons were treated with recombinant human oligomeric phospho-tau (Oligo-pTau) with or without antibodies. Cells were stained for human tau, MAP2, and murine IgG. MAP2 staining of dendrites (A), human tau (green) and MAP2 staining (B), and mouse IgG (magenta) and MAP2 staining (C) are shown. MAP2 signal in B and C was linearly and uniformly reduced in all images to better present the corresponding human tau or mouse IgG signal. Arrows indicate neuronal cell bodies that are lacking human-specific tau signal (B) or mouse IgG signal (C). Asterisks indicate human-specific tau (B) or mouse IgG (C) staining corresponding with MAP2-negative cells (non-neuronal cell types in hippocampal culture). Arrowheads indicate human tau-positive neuronal cell bodies. Scale bar, 20 μm.

(D) Automated quantification of MAP2 fragmentation.

Error bars represent SEM; *$p < 0.05$ by two-tailed Student's t test between indicated conditions; ns, not significant. Control, vehicle-buffer containing arachidonic acid and heparin; Con IgG, control IgG2a antibody; pS409 WT, anti-pS409 IgG2a WT antibody; pS409 DANG, anti-pS409 IgG2a DANG mutant. n for each condition is described in Table S2.

bind oligo-pTau extracellularly, preventing its uptake by neurons and consequently neutralizing its toxicity.

Effector Function Drives Antibody-Mediated Uptake of Extracellular Tau and Pro-inflammatory Cytokine Release by Cultured Microglia

Next, we determined the impact of antibody effector function on microglial uptake of extracellular tau. Microglia are the resident phagocytic immune cells of the CNS (Prinz and Priller, 2014), and our data show that microglia, but not neurons, express FcγRs. We therefore hypothesized that full effector antibodies would enhance uptake of extracellular tau via FcγR-mediated engulfment. Indeed, when oligo-pTau was added to the media of cultured microglia, it underwent internalization that was enhanced by anti-pS409-Tau WT, but not by anti-pS409-Tau DANG or IgG2a-control (Figures 6A and 6C). As expected, anti-pS409-Tau WT co-localized with oligo-pTau and FcγRs (Figure 6B), confirming FcγR-mediated uptake of antibody-tau complexes. In strong support of this finding, we detect only residual effectorless or IgG2a-control antibodies in microglia, and these do not localize with tau or FcγRs (Figure 6A).

Microglial engulfment of antibody-antigen complexes can trigger release of pro-inflammatory cytokines (Hanisch and Kettenmann, 2007; Prinz and Priller, 2014). Given the possible deleterious effects of chronic inflammation on neurons (Glass et al., 2010), we tested if full effector anti-Tau activates microglia. We measured interleukin 6 (IL-6), tumor necrosis factor α (TNF-α), and IL-1β in media collected from cultured primary microglia treated with different combinations of oligo-pTau and tau antibodies. We observed a significant increase in levels of all three cytokines upon exposure to oligo-pTau. The addition of anti-pS409-Tau WT dramatically increased cytokine levels even further, an increase that was not observed when anti-pS409-Tau DANG or IgG2a-control antibodies were added (Figures 6D–6F). Anti-pS409-tau WT alone had no effect on cytokine levels in the absence of oligo-pTau. These results show that effector function in the presence of target-bound anti-tau stimulates cytokine release. This cytokine release raises concern for possible deleterious effects in the CNS, reinforcing the rationale for mechanistic investigation of the role of effector function in efficacy and safety.

Only Effectorless, but Not Full Effector, Anti-pS409-Tau Protects Neurons from Oligo-pTau-Induced Toxicity in Neuron-Microglia Co-cultures

To directly test whether enhanced microglial activation by full effector anti-Tau could be deleterious to neurons, we generated neuron-microglia co-cultures and treated them with oligo-pTau

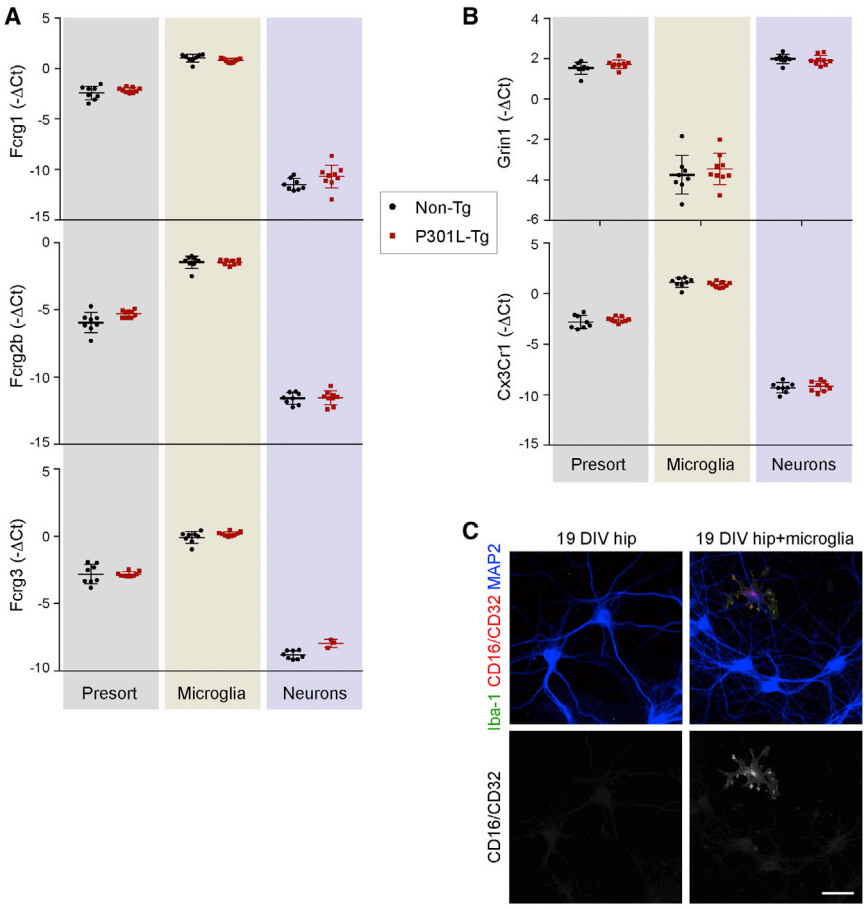

Figure 5. Fcγ Receptors Are Not Detectable in Neurons from Non-Tg or Tau P301L-Tg Hippocampi or in Cultured Hippocampal Neurons

(A) Fluidigm qPCR measurement of FcγR1 (top), FcγR2b (middle), and FcγR3 (bottom) expression levels in microglia and neurons purified and sorted by FACS from non-Tg and Tau P301L-Tg mouse hippocampi. No FcγR-expression was detected in neurons.

(B) Enrichment of specific cell types after FACS purification used in (A) was validated by measuring mRNA levels of the cell-type-specific genes Grin1 (neuron-specific, top) and Cx3Cr1 (microglia-specific, bottom) by Fluidigm qPCR analysis.

(C) 19 DIV embryonic hippocampal culture was fixed and stained for Iba-1 to detect microglia, with CD16/CD32 to detect FcγRs and MAP2 to visualize neurons. No FcγR staining was detected in neurons. However, primary-cultured microglia added to the hippocampal culture stained positive for CD16/CD32, confirming that FcγRs are expressed in microglia.

Scale bars, 20 μm. Error bars represent SD.

and antibodies. In the absence of microglia, both WT and DANG anti-pS409-Tau antibodies prevented oligo-pTau-mediated neuronal toxicity (Figures 7A, top row, 7B, and 4A). However, in the presence of microglia, anti-pS409-Tau WT was no longer protective, as evidenced by severe neuronal fragmentation. In contrast, the effectorless anti-pS409-Tau DANG remained protective (Figures 7A and 7B). Microglial uptake of oligo-pTau in the co-culture was strongly enhanced by anti-pS409-Tau WT, but not by anti-pS409-Tau DANG or IgG2a control (Figure 7C). These data suggest that the protective effect of anti-tau in blocking oligo-pTau-induced toxicity is lost due to microglial activation by full effector function anti-tau. The protective effect is retained, even in the presence of microglia, when effector function is removed. An effectorless tau antibody can therefore block spreading of tau pathology in vivo and protect neurons from direct tau-induced toxicity without activating microglia in vitro, properties that may be of significant importance for both safety and efficacy in the already inflamed environment of a degenerating AD brain.

DISCUSSION

Immunotherapy, particularly passive immunization, is a promising approach for disease-modifying treatments for Alzheimer's disease, based on extensive preclinical data for anti-amyloid and anti-tau, and emerging clinical data for anti-amyloids (Golde, 2014). Trials with amyloid-β-targeting antibodies have shown both the promise and potential risks of passive immunization. Notably, anti-amyloid therapies have been associated with ARIA only if the antibody has full effector function and binds oligomeric or fibrillar amyloid. Therefore, whether effector function is required for efficacy becomes a critical question when designing therapeutic antibodies. We show that a full effector anti-tau antibody enhances microglial uptake of extracellular tau in primary cultured microglia. These data agree with two recently published works showing that tau antibodies can promote microglial uptake and clearance of tau (Funk et al., 2015; Luo et al., 2015) and are consistent with the expression of FcγRs by microglia. In our study, we further investigated how this microglial uptake affects inflammatory responses and neuronal health. Importantly, we examined the role of antibody effector function in determining efficacy, both in vivo and in neuronal cultures, and show that effector function is not required for reducing accumulation of tau pathology in transgenic mice or for protection of cultured neurons from tau-mediated toxicity. Moreover, in neuron-microglia co-cultures exposed to extracellular toxic tau, only the effectorless anti-tau was protective, suggesting that while the full effector antibody enhances microglial uptake of tau, there could be a net negative impact of the antibody on adjacent neurons via activation of microglia. Based on our results, we propose that the primary protective mechanism of tau antibodies is the actual binding to extracellular tau, which prevents its uptake by neurons. This binding does not require effector function, since it does not involve the antibody Fc

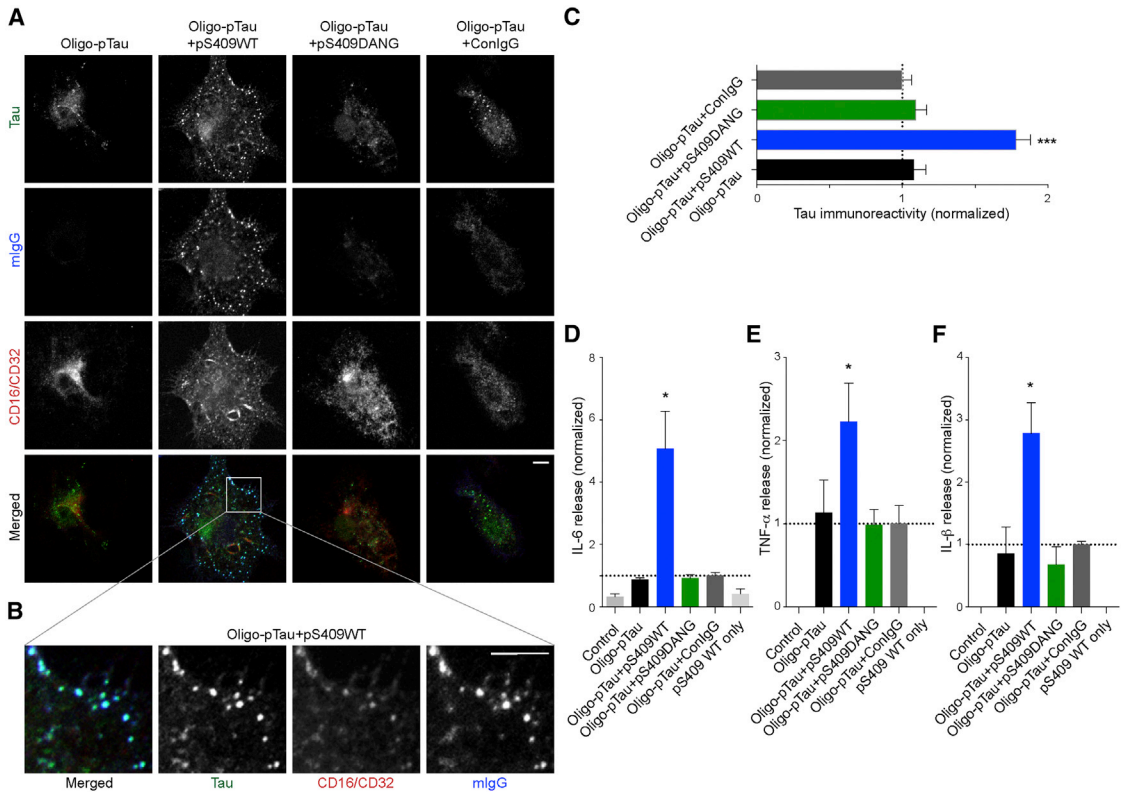

Figure 6. Effector Function Determines Antibody-Mediated Uptake of Recombinant Oligomeric Phospho-tau and Pro-inflammatory Cytokine Release by Cultured Microglia

Primary cultured microglia were incubated with oligomeric phospho-tau (Oligo-pTau) with and without antibodies.

(A) Microglia were incubated as indicated and imaged for tau (green), murine IgG (blue), and either Iba-1 (not depicted) or CD16/CD32 (red). Representative images of each condition are shown. Baseline oligo-pTau uptake by microglia is enhanced by pS409 WT, but not DANG, antibody, and only Tau taken up in presence of pS409 WT antibody co-localizes with muring IgG (mIgG) and FcγRs, suggesting FcγR-mediated uptake for pS409 WT antibody-Tau complexes only. Scale bar, 5 μm.

(B) High-magnification images of tau, CD16/CD32, and murine IgG in cells treated with oligo-pTau and pS409 WT. Scale bar, 5 μm.

(C) Quantification of tau immunoreactivity shows uptake of oligomeric tau by microglia is enhanced only by the full effector tau antibody. All values were normalized relative to Oligo-pTau+ConIgG. Error bars represent SEM. ***$p < 0.001$.

(D–F) Microglia were incubated at indicated conditions for 24 hr, and culture media were collected to measure IL-6 (D), TNF-α (E), and IL-1β (F) by ELISA. All values were normalized relative to Oligo-pTau+ConIgG. Error bars represent SEM. *$p < 0.05$.

n for each condition is indicated in Table S2.

p values by two-tailed Student's t test. Oligo-pTau, oligomeric phospho-tau; Control, vehicle-buffer containing arachidonic acid and heparin; Con IgG, control IgG2a antibody; pS409 WT, anti-pS409 IgG2a WT antibody; pS409 DANG, anti-pS409 IgG2a DANG mutant.

region. The antibody effector function status, however, may determine the downstream mechanisms of clearance after the binding of extracellular tau. Full effector antibodies promote FcγR-mediated uptake and clearance of tau by microglia. We show that this can consequently induce inflammatory responses in cultured microglia. The effectorless antibody, on the other hand, does not promote microglia-mediated uptake and therefore does not elicit microglial activation.

Our results suggest that tau antibodies do not target intracellular tau pathology. In vivo, we show that tau antibodies can slow the accumulation of tau pathology when it is still building up and spreading, but not at an older age when pathology has plateaued. If antibodies could target intracellular tau, we would expect to see clearance of existing pathology in treated older mice as well. A mechanism of action where neuronal FcγRs mediate antibody uptake by neurons, followed by engagement of intracellular tau tangles by the internalized antibody, has been previously proposed (Congdon et al., 2013; Gu et al., 2013). Possible reasons for the discrepancy between these studies and our work could be that in these published studies antibodies were applied ex vivo to sections of mouse brains, where the mechanical damage to cells and membranes during sectioning inevitably exposes intracellular pathology to extracellularly applied antibodies. Our results are based on efficacy studies in vivo with peripheral administration of the antibodies, an experimental paradigm that better models the treatment patients would receive in a clinical setting. The proposed mechanism of intracellular tau clearance by antibodies is based on an observation by IHC that neurons express FcγRs. However, non-specific signal is always a risk with this technique, especially when the antibody specificity has not been validated by lack of signal in knockout animal tissue. To address the questions of

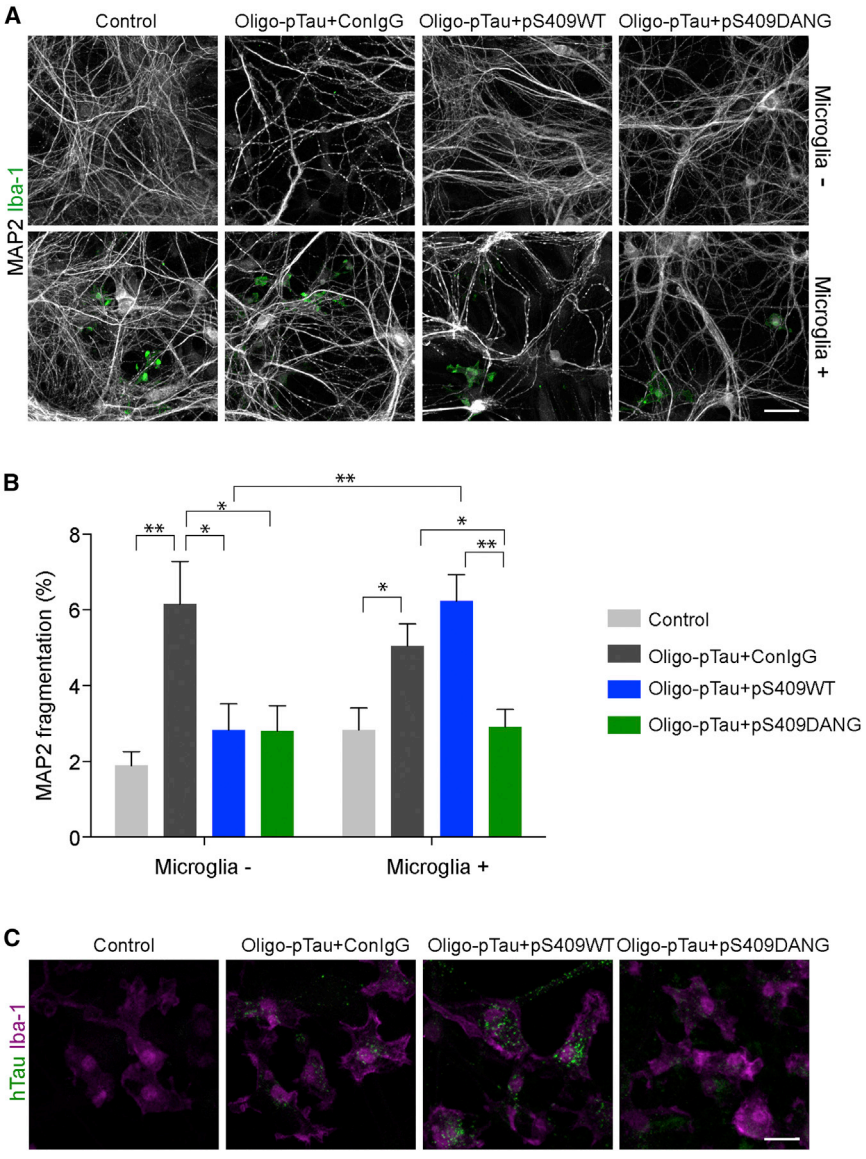

Figure 7. Only Effectorless, but Not Full Effector, Anti-pS409-Tau Protects Neurons from Oligo-pTau-Induced Toxicity in Neuron-Microglia Co-cultures

(A) Representative images of dendrites of neurons visualized by MAP2 staining (white) and microglia visualized by Iba-1 staining (green).

(B) Automated quantification of MAP2 fragmentation. Error bars represent SEM; *p < 0.05, **p < 0.01; two-tailed Student's t test. n for each condition is indicated in Table S2.

(C) Representative images of microglia (Iba-1) and oligo-phospho tau from each condition. Uptake of oligo-pTau by microglia is increased in the presence of anti-pS409 WT, but not DANG.

Scale bars, 20 μm. Control, vehicle-buffer containing arachidonic acid and heparin; Con IgG, control IgG2a antibody; pS409 WT, anti-pS409 IgG2a WT antibody; pS409 DANG, anti-pS409 IgG2a DANG mutant.

FcγR expression in neurons directly, we sorted neurons and microglia from WT and transgenic animals and found no detectable levels of mRNA to FcγRs in neurons. These results are in agreement with the online public transcriptome database of the WT mouse CNS (Zhang et al., 2014).

Anti-tau antibodies are less likely to cause vasogenic edema than amyloid-β-targeting antibodies given that NFTs are not associated with vasculature. A potential concern, however, arises from the inflammatory state of the brain in AD. It is not known if treatment with full effector anti-tau would further aggravate neuroinflammation in the diseased brain in a way that would offset the desired treatment effect of capturing and clearing extracellular tau. While providing an excellent model for accumulation of tau pathology, Tau P301L-Tg mice unfortunately do not recapitulate the widespread chronic neuroinflammation characteristic of Alzheimer's brains (Figure S6), which prevents us from testing our cell-based findings in vivo. Therefore, the in vitro risk we identify here may best predict potential adverse effects of full effector anti-tau antibodies in a brain with chronic inflammation. Importantly, amyloid-related imaging abnormalities showing vasogenic edema (ARIA-E) (Sperling et al., 2012) were not initially predicted in preclinical animal studies, yet they are a clear and present source of concern in currently ongoing anti-amyloid clinical trials in AD patients.

In summary, we show that effector function in anti-tau is not required for efficacy in vivo. Furthermore, both full effector-positive and effectorless anti-tau reduce the toxicity induced by oligo-pTau in primary neuron cultures. However, only full effector anti-tau drive microglial engulfment of tau, resulting in robust cytokine release, which is potentially deleterious to neurons. Indeed, we observed that in neuron-microglia co-cultures, full effector anti-tau induces neuronal toxicity while effectorless anti-tau remains protective against oligo-pTau-induced toxicity.

These results offer important preclinical mechanistic insights to anti-tau therapy, thus providing potential translational considerations when designing anti-tau therapies for clinical studies. Our findings may also be broadly applicable to antibody approaches for treating neurodegenerative diseases beyond tau.

EXPERIMENTAL PROCEDURES

Mice

Transgenic mice expressing human Tau P301L under the Thy1 promoter (Tau P301L-Tg) were previously described (Götz et al., 2001) and were maintained on a C57BL/6N (Charles River Laboratories) background. The protocols for in vivo mouse experiments were approved by the Genentech Institutional

Animal Care and Use Committee. All work was conducted according to NIH guidelines for the humane care and treatment of laboratory animals.

Generation of Anti-Tau-pS409 Antibody

Anti-pS409-Tau was generated by vaccinating WT C57BL/6 mice with a liposomal SupraAntigen vaccine (Muhs et al., 2007) modified to contain a palmitoylated peptide carrying the pS404 and pS409 tau phospho-epitopes. Splenocytes were fused with SP2/O-Ag14 myeloma cells, and the hybridoma expressing the antibody was isolated and expanded by limiting dilution. The specificity of the antibody to the Tau-pS409 epitope was verified with ELISA assays using multiple phospho- and nonphospho-peptides (Anawa Trading SA) and full-length human tau (tau-441; SignalChem) phosphorylated on the serine 409 site by a recombinant protein kinase A (PKA) catalytic subunit (New England Biolabs) at 12,525 U/ml. Further characterization was performed by western blot using full-length recombinant tau protein, unphosphorylated or phosphorylated with PKA at 2,088 U/ml (low PKA) or 12,525 U/ml (high PKA) (Figure 2). Anti-pS409-Tau was sequenced and variable regions cloned into WT and DANG murine IgG2a and murine kappa light-chain expression vectors.

Anti-pS409-Tau IgG2a WT and DANG were expressed in Chinese hamster ovary (CHO) cell line and purified by Protein A affinity chromatography, followed by size-exclusion chromatography to remove aggregate. Purity (> 95%) was verified by SDS-PAGE gel and size exclusion chromatography with multi-angle light scattering (SEC-MALLS). Identity of the antibodies was confirmed by mass spectroscopy. The endotoxin level was less than 0.5 EU/mg as measured by the limulus amebocyte lysate (LAL) assay.

Immunohistochemistry of Human Cortical Brain Sections

IHC was performed on 4um thick formalin-fixed, paraffin-embedded tissue sections mounted on glass slides. All IHC steps were carried out on the Ventana Discovery XT automated platform (Ventana Medical Systems). Sections were treated with Ventana Protease 2 for 8 min (Ventana Medical Systems) and then incubated in pS409 antibody at a working concentration of 0.05 μg/ml for 60 min at 37°C. Specifically bound primary antibody was detected by the OmniMap anti-mouse HRP detection for 16 min, followed by ChromoMap DAB (Ventana Medical Systems). The sections were counterstained with Hematoxylin II (Ventana Medical Systems), dehydrated, and coverslipped.

AlphaLISA of Human Cortical Brain Lysates

Details are provided in the Supplemental Experimental Procedures.

Antibody Treatment and Dosing

Tau P301L-Tg and WT littermate mice were assigned to treatment groups and dosed once weekly intraperitoneally (i.p.) with IgG2a-control (anti-ragweed) at 30 mg/kg; anti-pS409-Tau WT IgG2a at 3, 10, or 30 mg/kg; or anti-pS409-Tau DANG IgG2a at 3 or 30 mg/kg. All antibody dosing solutions were prepared in 10 mM histidine (pH 5.8), 6% sucrose, and 0.02% Tween 20 at a concentration of 10 mg/ml. Treatment started at 13 weeks of age. The groups in the in vivo study were balanced for sex and litter and staggered into four cohorts. In addition, three TauP301L-Tg mice were harvested at age 3 months without undergoing any treatment in order to determine the baseline level of pathology at the time of treatment initiation. Refer to Table S1 for detailed description of total n by treatment, genotype, and sex.

Mouse Tissue Harvest

Mice were anesthetized with 2.5% tribromoethanol (0.5 ml per 25 g body weight) and transcardially perfused with PBS. Brains were harvested and bisected. Right hemispheres were fixed in 4% paraformaldehyde overnight at 4°C then transferred to PBS prior to processing for immunohistochemistry. Left hemispheres were sub-dissected on ice then frozen at −80°C for biochemical analysis. Tail clips were taken from all mice to confirm genotypes. Cerebella and plasma were harvested and used for antibody exposure analysis (see the Supplemental Experimental Procedures).

Mouse Brain Section Preparation and Immunohistochemistry

For model characterization (Figures 1A and 1B) and aged in vivo study (Figure S3), hemibrains were sectioned at 35 μm thickness as free-floating sections. For the efficacy study (Figure 3), brains were embedded into a gelatin matrix using MultiBrain blocks (NeuroScience Associates) and sectioned sagittally at 25 μm thickness. Each sex was represented on separate blocks, but within each block, the brain position was randomized relative to genotype and treatment.

Free-floating sections of individual mouse hemibrains or of MultiBrain blocks were stained as previously described (Le Pichon et al., 2013) but with washes in PBS instead of Tris buffered saline and primary antibody incubations at 4°C instead of room temperature. Primary antibodies included: rabbit anti-pTau212/214 (generated in-house; 0.01 μg/ml, Figure S7), mouse IgG3 antibody PG-5 (Peter Davies, AECOM, 1:300), anti-tau HT7 (MN1000, Thermo Scientific, 1:1,000), rat anti-CD68 (clone FA-11, MCA1957, Serotec, 1:800). To avoid high background staining, in the case of mouse primary antibodies that were subtype specific, we used the corresponding subtype-specific secondary antibody (e.g., biotinylated anti-mouse IgG3, Bethyl A90-111B).

IHC Quantification

Immunohistochemically stained slides were imaged using the Leica SCN400 (Leica Microsystems) whole-slide scanning system at 200× magnification with a resolution of 0.5 μm/pixel. Regions of interest (ROIs) were manually drawn on four matched hippocampal levels per animal, and the amount of staining in these ROIs was quantified in an automated fashion using the two endpoints described below. All image analysis was performed blind to genotype and treatment groups.

Positive Pixel Area Analysis for Quantitation of IHC Stains

Digital images of antibody-labeled brain sections were analyzed as previously described (Le Pichon et al., 2013). The percent area stained was calculated by normalizing the total positive pixels to the total pixel area of the ROI.

Integrated Intensity

Integrated intensity was calculated using the Beer-Lambert law, absorbance = −log(transmitted light intensity/incident light intensity), for the positive pixel areas only.

Biochemical Characterization of Tau P301L-Tg Mice

Details are provided in the Supplemental Experimental Procedures.

Biochemical Analysis and Quantification of Efficacy Studies

Left hemispheres from Tau-P301L-Tg or WT littermates were subdissected and hippocampi were homogenized in 200 μl TBS (50 mM Tris [pH 7.4], 150 mM NaCl, 2 mM EGTA, Complete Mini and PhosSTOP) using TissueLyser. The lysates were centrifuged at 14,000 × *g* (12,000 rpm) for 10 min at 10°C to separate supernatant (S1) and pellet (P1). S1 was further centrifuged at 180,000 × *g* (55,000 rpm) for 1 hr at 20°C. The supernatants (S2) were carefully removed and the pellets (P2) were resuspended in 50 μl of 1% sarkosyl-containing TBS and sonicated. Following protein measurement by BCA, P2 lysates were mixed with SDS-PAGE loading buffer and boiled, and 5 μg (for total tau) or 15 μg (for phospho-tau) protein lysates were subjected to SDS-PAGE, transfer, and incubation with primary antibodies (anti-tau, A0024, DAKO; AT8, MN1020, Thermo Scientific, and rabbit polyclonal anti-pT212pS214, described above) at 4°C overnight followed by incubation with fluorescence-conjugated secondary antibodies (LI-COR). Fluorescence was detected with an Odyssey scanner (LI-COR). The intensities of bands at the molecular weight of human tau (60–70 KDa), and β-actin bands were measured with the integrated LI-COR analysis software.

Generation of Recombinant Tau and Oligomeric Phosphorylated Tau

Details are provided in the Supplemental Experimental Procedures.

Primary Hippocampal and Microglial Cultures

Details are provided in the Supplemental Experimental Procedures.

Hippocampal-Microglial Co-cultures

Hippocampal-microglial co-cultures were prepared by replating microglia dissociated from 225-mm^2 culture flasks onto 18 days in vitro (DIV) primary hippocampal neurons in eight-well slide chambers (12,500 microglia and

25,000 neurons per one well). Co-cultures were treated with recombinant tau and antibodies 4 hr after microglia plating.

In Vitro Treatment with Recombinant Tau and Antibodies

For 18 DIV hippocampal cultures or hippocampal-microglial co-cultures, recombinant human oligomeric phospho-tau and antibodies (500 nM each at 1:1 ratio) or controls were pre-incubated in neuron culture medium (conditioned medium from 18 DIV hippocampal culture:fresh NbActiv4 at 1:1) for 1 hr at 37°C before they were added to the cells. Cells were incubated with the tau-antibody mix or control in the media for 72 hr (hippocampal cultures) or 48 hr (hippocampal-microglial co-cultures). Cells were washed with PBS three times before fixation.

For microglia cultures, recombinant human oligomeric phospho-tau and antibodies or controls were pre-incubated at 500 nM each (immunocytochemistry/imaging) or 250 nM each (cytokine assay) in low-glucose DMEM in the absence of serum for 1 hr at 37°C prior to the addition to the cells. For immunocytochemistry and imaging, cells were incubated with the tau-antibody mix or controls for 10 min and washed three times with PBS before fixation. For cytokine assay, cells were incubated with the tau-antibody mix or control for 24 hr and medium of each well was collected for cytokine assay.

Immunocytochemistry

Details are provided in the Supplemental Experimental Procedures.

Confocal Imaging and Quantification

Confocal fluorescent imaging was performed with a LSM780 (Carl Zeiss) using Zen 2010 software (Carl Zeiss). For imaging of hippocampal cultures and hippocampal-microglial co-cultures, 5 z-stack images at 0.98-μm intervals were collected using a Plan-Apochromat 20×/0.8 M27 objective lens. For the MAP2 fragmentation assay, a maximum intensity z projection was created for the image stack and analyzed using Metamorph (Molecular Devices). A median filter and nearest-neighbor deconvolution were used for noise reduction. Neurite and cell body lengths were analyzed using the neurite outgrowth module followed by morphological processing. Fragments less than 15 pixels (6.225 μm) were normalized to total signal length to obtain a measure of MAP2 fragmentation.

Microglia were imaged with an α-Plan-Apochromat 100×/1.46 M27 objective. Quantification of recombinant tau uptake in the cells was performed with ImageJ (1.43u, 64-bit, NIH). ROIs of cell area were drawn manually using Iba-1 signal as a reference. Area and integrated intensity of tau immunoreactivity of ROIs were measured to obtain tau immunoreactivity normalized to area. All analyses were performed blinded to experimental conditions.

Sorting of Mouse Brain Cells and qPCR

For flow cytometry sorting (fluorescence-activated cell sorting [FACS]) of adult mouse hippocampi (5–10 months old), both hippocampi per (n = 9 Tau-P301L-Tg, n = 7 non-Tg) were dissected and dissociated in 1.5 ml Accutase (#SCr005, Millipore) for 20 min at 4°C. The tissues were triturated to single cell suspension in Hibernate-A LF (BrainBits, LLC), passed through a Percoll gradient, resuspended, fixed in ethanol, and labeled with primary antibodies: NeuN-488 (MAB377X, 1:1,000, Millipore) and CD11b-APC (551282, 1:250, BD Biosciences) for 30 min at 4°C. DAPI was added to gate on single cells. The cell-specific subtypes (including "presort," defined as DAPI+ cells collected before sorting into the cell-type specific fluorescent gates) were isolated by FACS and collected for qPCR analysis by Fluidigm. Expression levels of individual genes assayed were normalized to the geometric mean of 3 stably expressed genes (*ACTB*, *GAPDH*, and *HPRT*) for each sample (ΔCt). Negative ΔCts are plotted. Enrichment of each cell type by FACS was validated by qPCR of cell-type-specific markers (Figure 5B). Because there were no sex effects or age effects observed with qPCR results, sex and age were pooled in the presented data (Figures 5A and 5B).

Cytokine ELISA

Details are provided in the Supplemental Experimental Procedures.

Statistical Analysis

All data collected from mouse studies, including immunohistochemistry and western blotting, were plotted and analyzed using JMP (Version 10.0.2, SAS Institute). Two-way ANOVA was used to assess dose level effects, calculated using a whole model regression analysis with sex, dose level, and the interaction of sex and dose level as factors. There was no effect of sex or any interaction between sex and dose level in these studies. Two-tailed Student's t test was used to compare each of the treatment groups with a single control. Data from cell culture experiments were plotted and analyzed with Microsoft Excel 2008 and Prism (version 6.0f, GraphPad). Two-tailed Student's t test was used to compare each pair of conditions. For all analyses of in vivo and in vitro data, error bars represent SEM (except Figure 5, where error bars represent SD; $^{*}p < 0.05$, $^{**}p < 0.01$, and $^{***}p < 0.001$).

SUPPLEMENTAL INFORMATION

Supplemental Information includes Supplemental Experimental Procedures, seven figures, and three tables and can be found with this article online at http://dx.doi.org/10.1016/j.celrep.2016.06.099.

AUTHOR CONTRIBUTIONS

S.-H.L., C.E.L.P., O.A., V.G., M.P., H.L., H.S., R.B., H.N., R.C., D.D., K.S., D.B., and G.A. conducted experiments; S.-H.L., C.E.L.P., O.A., M.P., O.F., J.A.E., D.D., I.H., K.S., D.V.H., J.A., Y.L., D.B., A.P., A.M., R.J.W., K.S.-L., and G.A. designed the experiments; and S.-H.L., C.E.L.P., R.J.W., K.S.-L., and G.A. wrote the paper.

ACKNOWLEDGMENTS

We thank Melissa Gonzalez-Edick and Jeffrey Eastham-Anderson for assistance with whole-slide scanning and workflow management. Authors are full-time employees of Genentech, Inc., AC Immune SA, or Gilead Sciences.

Received: November 24, 2015
Revised: May 27, 2016
Accepted: June 29, 2016
Published: July 28, 2016

REFERENCES

Adolfsson, O., Pihlgren, M., Toni, N., Varisco, Y., Buccarello, A.L., Antoniello, K., Lohmann, S., Piorkowska, K., Gafner, V., Atwal, J.K., et al. (2012). An effector-reduced anti-β-amyloid (Aβ) antibody with unique aβ binding properties promotes neuroprotection and glial engulfment of Aβ. J. Neurosci. *32*, 9677–9689.

Boutajangout, A., Ingadottir, J., Davies, P., and Sigurdsson, E.M. (2011). Passive immunization targeting pathological phospho-tau protein in a mouse model reduces functional decline and clears tau aggregates from the brain. J. Neurochem. *118*, 658–667.

Braak, H., and Braak, E. (1991). Neuropathological stageing of Alzheimer-related changes. Acta Neuropathol. *82*, 239–259.

Braak, H., and Braak, E. (1995). Staging of Alzheimer's disease-related neurofibrillary changes. Neurobiol. Aging *16*, 271–278, discussion 278–284.

Chai, X., Wu, S., Murray, T.K., Kinley, R., Cella, C.V., Sims, H., Buckner, N., Hanmer, J., Davies, P., O'Neill, M.J., et al. (2011). Passive immunization with anti-Tau antibodies in two transgenic models: reduction of Tau pathology and delay of disease progression. J. Biol. Chem. *286*, 34457–34467.

Chai, X., Dage, J.L., and Citron, M. (2012). Constitutive secretion of tau protein by an unconventional mechanism. Neurobiol. Dis. *48*, 356–366.

Congdon, E.E., Gu, J., Sait, H.B., and Sigurdsson, E.M. (2013). Antibody uptake into neurons occurs primarily via clathrin-dependent Fcγ receptor endocytosis and is a prerequisite for acute tau protein clearance. J. Biol. Chem. *288*, 35452–35465.

Couch, J.A., Yu, Y.J., Zhang, Y., Tarrant, J.M., Fuji, R.N., Meilandt, W.J., Solanoy, H., Tong, R.K., Hoyte, K., Luk, W., et al. (2013). Addressing safety liabilities of TfR bispecific antibodies that cross the blood-brain barrier. Sci. Transl. Med. *5*, 183ra57, 1–12.

d'Abramo, C., Acker, C.M., Jimenez, H.T., and Davies, P. (2013). Tau passive immunotherapy in mutant P301L mice: antibody affinity versus specificity. PLoS ONE *8*, e62402.

de Calignon, A., Polydoro, M., Suárez-Calvet, M., William, C., Adamowicz, D.H., Kopeikina, K.J., Pitstick, R., Sahara, N., Ashe, K.H., Carlson, G.A., et al. (2012). Propagation of tau pathology in a model of early Alzheimer's disease. Neuron *73*, 685–697.

Funk, K.E., Mirbaha, H., Jiang, H., Holtzman, D.M., and Diamond, M.I. (2015). Distinct therapeutic mechanisms of Tau antibodies: promoting microglial clearance versus blocking neuronal uptake. J. Biol. Chem. *290*, 21652–21662.

Glass, C.K., Saijo, K., Winner, B., Marchetto, M.C., and Gage, F.H. (2010). Mechanisms underlying inflammation in neurodegeneration. Cell *140*, 918–934.

Goedert, M., Ghetti, B., and Spillantini, M.G. (2012). Frontotemporal dementia: implications for understanding Alzheimer disease. Cold Spring Harb. Perspect. Med. *2*, a006254.

Golde, T.E. (2014). Open questions for Alzheimer's disease immunotherapy. Alzheimers Res. Ther. *6*, 3.

Götz, J., Chen, F., Barmettler, R., and Nitsch, R.M. (2001). Tau filament formation in transgenic mice expressing P301L tau. J. Biol. Chem. *276*, 529–534.

Gu, J., Congdon, E.E., and Sigurdsson, E.M. (2013). Two novel Tau antibodies targeting the 396/404 region are primarily taken up by neurons and reduce Tau protein pathology. J. Biol. Chem. *288*, 33081–33095.

Hanisch, U.K., and Kettenmann, H. (2007). Microglia: active sensor and versatile effector cells in the normal and pathologic brain. Nat. Neurosci. *10*, 1387–1394.

Iba, M., Guo, J.L., McBride, J.D., Zhang, B., Trojanowski, J.Q., and Lee, V.M. (2013). Synthetic tau fibrils mediate transmission of neurofibrillary tangles in a transgenic mouse model of Alzheimer's-like tauopathy. J. Neurosci. *33*, 1024–1037.

Jicha, G.A., O'Donnell, A., Weaver, C., Angeletti, R., and Davies, P. (1999). Hierarchical phosphorylation of recombinant tau by the paired-helical filament-associated protein kinase is dependent on cyclic AMP-dependent protein kinase. J. Neurochem. *72*, 214–224.

Kfoury, N., Holmes, B.B., Jiang, H., Holtzman, D.M., and Diamond, M.I. (2012). Trans-cellular propagation of Tau aggregation by fibrillar species. J. Biol. Chem. *287*, 19440–19451.

Kimura, T., Ono, T., Takamatsu, J., Yamamoto, H., Ikegami, K., Kondo, A., Hasegawa, M., Ihara, Y., Miyamoto, E., and Miyakawa, T. (1996). Sequential changes of tau-site-specific phosphorylation during development of paired helical filaments. Dementia *7*, 177–181.

Le Pichon, C.E., Dominguez, S.L., Solanoy, H., Ngu, H., Lewin-Koh, N., Chen, M., Eastham-Anderson, J., Watts, R., and Scearce-Levie, K. (2013). EGFR inhibitor erlotinib delays disease progression but does not extend survival in the SOD1 mouse model of ALS. PLoS ONE *8*, e62342.

Leabman, M.K., Meng, Y.G., Kelley, R.F., DeForge, L.E., Cowan, K.J., and Iyer, S. (2013). Effects of altered FcγR binding on antibody pharmacokinetics in cynomolgus monkeys. MAbs *5*, 896–903.

Liu, L., Drouet, V., Wu, J.W., Witter, M.P., Small, S.A., Clelland, C., and Duff, K. (2012). Trans-synaptic spread of tau pathology in vivo. PLoS ONE *7*, e31302.

Luo, W., Liu, W., Hu, X., Hanna, M., Caravaca, A., and Paul, S.M. (2015). Microglial internalization and degradation of pathological tau is enhanced by an anti-tau monoclonal antibody. Sci. Rep. *5*, 11161.

Mandelkow, E.M., and Mandelkow, E. (2012). Biochemistry and cell biology of tau protein in neurofibrillary degeneration. Cold Spring Harb. Perspect. Med. *2*, a006247.

Muhs, A., Hickman, D.T., Pihlgren, M., Chuard, N., Giriens, V., Meerschman, C., van der Auwera, I., van Leuven, F., Sugawara, M., Weingertner, M.C., et al. (2007). Liposomal vaccines with conformation-specific amyloid peptide antigens define immune response and efficacy in APP transgenic mice. Proc. Natl. Acad. Sci. USA *104*, 9810–9815.

Ostrowitzki, S., Deptula, D., Thurfjell, L., Barkhof, F., Bohrmann, B., Brooks, D.J., Klunk, W.E., Ashford, E., Yoo, K., Xu, Z.X., et al. (2012). Mechanism of amyloid removal in patients with Alzheimer disease treated with gantenerumab. Arch. Neurol. *69*, 198–207.

Prinz, M., and Priller, J. (2014). Microglia and brain macrophages in the molecular age: from origin to neuropsychiatric disease. Nat. Rev. Neurosci. *15*, 300–312.

Shaw, L.M., Vanderstichele, H., Knapik-Czajka, M., Clark, C.M., Aisen, P.S., Petersen, R.C., Blennow, K., Soares, H., Simon, A., Lewczuk, P., et al.; Alzheimer's Disease Neuroimaging Initiative (2009). Cerebrospinal fluid biomarker signature in Alzheimer's disease neuroimaging initiative subjects. Ann. Neurol. *65*, 403–413.

Skovronsky, D.M., Lee, V.M., and Trojanowski, J.Q. (2006). Neurodegenerative diseases: new concepts of pathogenesis and their therapeutic implications. Annu. Rev. Pathol. *1*, 151–170.

Sperling, R., Salloway, S., Brooks, D.J., Tampieri, D., Barakos, J., Fox, N.C., Raskind, M., Sabbagh, M., Honig, L.S., Porsteinsson, A.P., et al. (2012). Amyloid-related imaging abnormalities in patients with Alzheimer's disease treated with bapineuzumab: a retrospective analysis. Lancet Neurol. *11*, 241–249.

Wyss-Coray, T., and Rogers, J. (2012). Inflammation in Alzheimer disease-a brief review of the basic science and clinical literature. Cold Spring Harb. Perspect. Med. *2*, a006346.

Yamada, K., Cirrito, J.R., Stewart, F.R., Jiang, H., Finn, M.B., Holmes, B.B., Binder, L.I., Mandelkow, E.M., Diamond, M.I., Lee, V.M., and Holtzman, D.M. (2011). In vivo microdialysis reveals age-dependent decrease of brain interstitial fluid tau levels in P301S human tau transgenic mice. J. Neurosci. *31*, 13110–13117.

Yanamandra, K., Kfoury, N., Jiang, H., Mahan, T.E., Ma, S., Maloney, S.E., Wozniak, D.F., Diamond, M.I., and Holtzman, D.M. (2013). Anti-tau antibodies that block tau aggregate seeding in vitro markedly decrease pathology and improve cognition in vivo. Neuron *80*, 402–414.

Yu, Y.J., and Watts, R.J. (2013). Developing therapeutic antibodies for neurodegenerative disease. Neurotherapeutics *10*, 459–472.

Zhang, Y., Chen, K., Sloan, S.A., Bennett, M.L., Scholze, A.R., O'Keeffe, S., Phatnani, H.P., Guarnieri, P., Caneda, C., Ruderisch, N., et al. (2014). An RNA-sequencing transcriptome and splicing database of glia, neurons, and vascular cells of the cerebral cortex. J. Neurosci. *34*, 11929–11947.